21st European Workshop on White Dwarfs
Castanheira, Vanderbosch, Montgomery, eds.
July 23–27, 2018, Austin, Texas, USA

Evolutionary and pulsational properties of ultra-massive white dwarfs. The role of oxygen-neon phase separation.

F. C. De Gerónimo,[1,2], M. E. Camisassa[1,2], A. H. Córsico[1,2], L. G. Althaus,[1,2]

[1] Facultad de Ciencias Astronómicas y Geofísicas, Universidad Nacional de La Plata, Paseo del Bosque s/n, (1900) La Plata, Argentina; fdegeronimo@fcaglp.unlp.edu.ar
[2] Instituto de Astrofísica La Plata, CONICET-UNLP

Abstract

Ultra-massive hydrogen-rich white dwarfs (WDs) are expected to harbor oxygen/neon cores resulting from semi-degenerate carbon burning when the progenitor star evolves through the super asymptotic giant branch (SAGB) phase. These stars are expected to be crystallized by the time they reach the ZZ Ceti domain. We show that crystallization leads to a phase separation of oxygen and neon in the core of ultra-massive WDs, which impacts markedly the pulsational properties, thus offering a unique opportunity to study the processes of crystallization and to infer the core chemical composition in WD stars.

1 Methodology & input physics

We computed the evolution (Camisassa et al., 2018) and pulsation properties (De Gerónimo et al., 2018) of ultra-massive DA (hydrogen-rich) WD sequences with stellar masses $M_\star = 1.10, 1.16, 1.22$, and $1.29 M_\odot$ (Fig. 1) resulting from the complete evolution of the progenitor stars through the SAGB phase (Siess, 2010). Prior evolution provides us with realistic core chemical profiles, envelope stratification and helium mass. In table 1 we show the He mass of our models, together with the effective temperature and surface gravity at the onset of crystallization, and the fraction of crystallized mass at the blue and red edges of the ZZ Ceti instability strip. The cores are composed mostly of ^{16}O and ^{20}Ne, and smaller amounts of ^{12}C, ^{23}Na and ^{24}Mg. The H content is set to $M_{\rm H} \sim 10^{-6} M_\star$.

Nonradial g-mode (gravity mode) pulsations of our complete set of ultra-massive ONe-core DA WD models were computed using the adiabatic version of the LP-PUL pulsation code (Córsico et al., 2005). The pulsation code is based on the general Newton-Raphson technique that solves the full fourth order set of equations and boundary conditions governing linear, spheroidal, adiabatic, non-radial stellar pulsations following the dimensionless formulation of Dziembowski (1971). To account for the effects of crystallization on the pulsation spectrum of g modes, we adopted the "hard sphere" boundary conditions, which assume that the amplitude of the eigenfunctions of g modes is drastically reduced below the solid/liquid interface due to the non-zero shear modulus of the solid, as compared with the amplitude in the fluid region (see Montgomery & Winget, 1999).

The DA WD evolutionary models developed in this work were computed with the amply used LPCODE evolutionary code (Althaus et al., 2005). This code considers all the physical ingredients involved in WD, including element diffusion. In this work we included, *for the first time*, both energy release and chemical abundance changes caused by the process of phase separation during crystallization. We considered the phase diagram of Medin & Cumming (2010), suitable for the dense plasma of oxygen/neon mixtures appropriate for ultra-massive WDs. We computed an additional sequence of CO-core WDs with $M_\star = 1.10 M_\odot$, for which crystallization was considered following the phase diagram of Horowitz et al. (2010). Phase diagrams provide us with the temperature at which crystallization occurs and the resulting abundances of the solid phase. To our knowledge, this is the *first* evolutionary and pulsational analysis of ultra-massive DA WD models that includes phase separation processes in ONe cores.

2 Results

In Fig. 1 we show the $\log g - T_{\rm eff}$ plane of our WD sequences, computed for this work. In addition, we plot the isochrones of 0.1, 0.5, 1, 2 and 5 Gyr (blue lines) together with the sample of ultra-massive DA WDs known to date (black plus symbols) and ultra-massive ZZ Ceti stars (red squares). It can be seen a change of slope of the isochrones, reflecting the dependence of cooling times on the mass of the WD: at early stages, evolution proceeds slower in more massive WDs, while the opposite trend is found at advanced stages.

We found that phase separation during crystallization strongly modifies the core chemical profiles of our

$M_\star/M_\odot$	$M_{\rm He}/M_\star$ $(\times 10^{-5})$	$T_{\rm eff}^{\rm c}$ (K)	$\log g^{\rm c}$ (cgs)	$M_{\rm c}/M_\star$ $(T_{\rm eff} = 12\,500$ K)	$M_{\rm c}/M_\star$ $(T_{\rm eff} = 10\,500$ K)
1.098	29.6	19881	8.83	0.81	0.92
1.159	15.7	23291	8.95	0.90	0.96
1.226	6.38	28425	9.12	0.96	0.98
1.292	1.66	37309	9.33	0.994	0.998

Table 1: He mass content of our ONe-core ultra-massive DA WD models, together with the effective temperature and surface gravity at the onset of crystallization, and the fraction of crystallized mass at the blue and red edges of the ZZ Ceti instability strip.

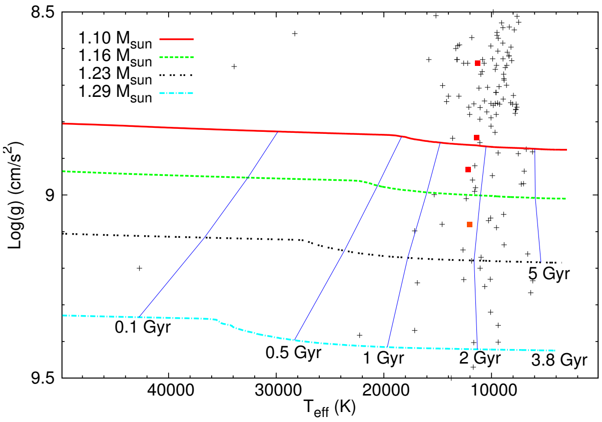

Figure 1: Hydrogen-rich WD model sequences in the $\log g - T_{\rm eff}$ plane. Blue solid lines display isochrones of 0.1, 0.5, 1, 2, and 5 Gyr. Plus symbols indicate the location of a sample of ultra-massive DA WDs. Squares display ultra-massive ZZ Ceti stars.

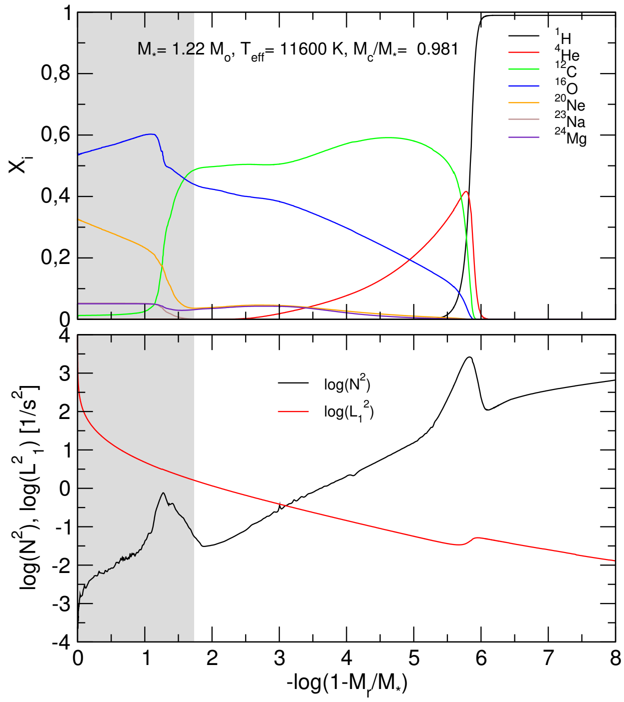

Figure 2: Chemical profiles (upper panel), and the logarithm of the squared Brunt-Väisälä and Lamb ($\ell = 1$) frequencies (lower panel), corresponding to a ONe-core WD model with $M_\star = 1.22 M_\odot$ and $T_{\rm eff} \sim 11\,600$ K. The gray area marks the domain of crystallization. $M_c/M_\star$ is the crystallized mass fraction of the model.

models, and this has a non-negligible impact on the period spectrum. Fig. 2 displays the chemical profiles and the logarithm of the squared Brunt-Väisälä and Lamb ($\ell = 1$) frequencies in terms of the outer mass fraction corresponding to a ONe-core WD model with $M_\star = 1.16 M_\odot$ and $T_{\rm eff} \sim 11\,600$ K and a percentage of crystallized mass of 98 %. Note that for this model, phase separation of ^{16}O and ^{20}Ne has already finished, and the triple chemical transition region C/O/Ne is located at $-\log(1 - M_r/M_\star) \sim 1.3$, well within the crystallized region. By virtue of this, the bump in the Brunt-Väisälä frequency associated to this chemical interface (see lower panel) is completely irrelevant for the pulsation properties of the model, since the g modes cannot propagate in the crystallized core. This implies that the only relevant chemical interface of the model is that of the ^{1}H and ^{4}He, located at $-\log(1 - M_r/M_\star) \sim 5.8$.

To explore the possibility of determining the core composition of ultra-massive ZZ Ceti stars through their pulsations, we have compared the period-spacing diagrams of CO-core and ONe-core WD models with $1.10 M_\odot$ and the same effective temperature. In Fig. 3 we depict the period spacing ($\Delta\Pi$) in terms of the pe-

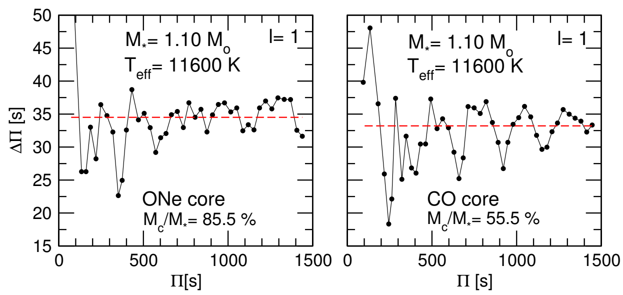

Figure 3: Forward period spacing ($\Delta\Pi$) in terms of the periods of $\ell = 1$ pulsation g modes for $1.10 M_\odot$ WD models at $T_{\rm eff} \sim 11600$ K with an ONe core (left panel) and a CO core (right panel). The percentages of the crystallized mass are indicated. The horizontal red-dashed line is the asymptotic period spacing.

riods of $\ell = 1$ pulsation g modes for two WD models at $T_{\rm eff} \sim 11600$ K with an ONe core (left) and a CO core (right). In both models, latent-heat release and chemical redistribution caused by phase separation have been taken into account during crystallization. We found that period-spacing departures from the mean period separation due to mode-trapping effects are smaller for the ONe-core model than for the CO-core model. We conclude that the features found in the period-spacing diagrams could be employed to differentiate the chemical composition of the cores of ultra-massive ZZ Ceti stars.

3 Conclusions

We found that phase separation during crystallization in the core of ultra-massive DA WDs has a marked impact on the pulsation properties of ultra-massive ZZ Ceti stars. Interestingly enough, we found that the differences in the period-spacing diagrams could be employed to infer the core composition of ultra-massive ZZ Ceti stars, something that should be complemented with detailed asteroseismic analyses using the individual observed periods. Promising targets to to achieve this goal are the ZZ Ceti stars BPM 37093 (Kanaan et al., 1992, 2005), GD 518 (Hermes et al., 2013), and SDSS J0840+5222 (Curd et al., 2017).

Acknowledgments

F.C.D.G and A.H.C. warmly thank the Local Organizing Committee of the 21st European White Dwarf Workshop for support that allowed him to attend this conference.

The evolutionary sequences presented in this work can be found at: `http://evolgroup.fcaglp.unlp.edu.ar/TRACKS/DA.html`

References

Althaus L. G., Serenelli A. M., Panei J. A., Córsico A. H., García-Berro E., Scóccola C. G., 2005, A&A, 435, 631

Camisassa M. E., et al., 2018, preprint, (arXiv:1807.03894)

Córsico A. H., Althaus L. G., Montgomery M. H., García-Berro E., Isern J., 2005, A&A, 429, 277

Curd B., Gianninas A., Bell K. J., Kilic M., Romero A. D., Allende Prieto C., Winget D. E., Winget K. I., 2017, MNRAS, 468, 239

De Gerónimo F. C., Córsico A. H., Althaus L. G., Wachlin F. C., Camisassa M. E., 2018, preprint, (arXiv:1807.03810)

Dziembowski W. A., 1971, Acta Astron., 21, 289

Hermes J. J., Kepler S. O., Castanheira B. G., Gianninas A., Winget D. E., Montgomery M. H., Brown W. R., Harrold S. T., 2013, ApJ, 771, L2

Horowitz C. J., Schneider A. S., Berry D. K., 2010, Physical Review Letters, 104, 231101

Kanaan A., Kepler S. O., Giovannini O., Diaz M., 1992, ApJ, 390, L89

Kanaan A., et al., 2005, A&A, 432, 219

Medin Z., Cumming A., 2010, Phys. Rev. E, 81, 036107

Montgomery M. H., Winget D. E., 1999, ApJ, 526, 976

Siess L., 2010, A&A, 512, A10